Extended modifications of electronic structures caused by defects: Scanning tunneling microscopy of graphite

Zhao Y. Rong
Physics Department, State University of New York–Stony Brook, Stony Brook, New York 11794
(Received 22 March 1994)

Electronic effects from two well-defined defects are identified and measured using scanning tunneling microscopy on graphite. An atomic vacancy on the topmost (0001) plane caused a lowering of apparent z height in a 30 Å×30 Å area by ~1.5 Å. A plane rotation relative to the third surface layer caused a Moiré pattern, with an attenuation along the c axis about 2.6 per monolayer. A "supervacancy" was imaged due to competition between the above two effects. An explanation based on changes in density of states near the Fermi level is proposed.

Graphite consists of hexagonal layers of sp^2 sites, weakly bonded together by van der Waals forces into an $ABAB$ stacking sequence along the c axis. Its electronic properties near the Fermi level are determined by delocalized π states, which has attracted much research for decades.[1] The graphite monolayer is a zero-gap semiconductor in which a single state at the corner of the surface Brillouin zone determines the Fermi energy that results in a standing wave of electron density along the plane.[2] The interlayer interactions cause a band overlap and shift wave functions concentrated on the A atoms (above atoms in the layer below) away from the Fermi energy. That introduces an asymmetry for the neighboring two atoms in a surface unit cell.[3] These unusual electronic structures were used to interpret the two anomalies of graphite, i.e., giant corrugations and the asymmetry, observed in scanning tunneling microscopy (STM), a technique which probes the local density of states at the Fermi level of a sample surface.[4] Moreover, the electronic properties of graphite are subject to change when the basic AB-stacked Bernal structure is modified[5] or intercalated,[6] and the electrical conductivity of the resulting material can vary from insulator to superconductor. Understanding the correlation between electronic structures and atomic-structure modifications of graphite is crucial for engineering these materials. Tunneling spectra and atomic images provided by STM are ideal approaches for studying the correlation. Indeed, STM studies have revealed many defect-related anomalies on graphite, which, in practice, complicate the interpretation of the images, especially when graphite is used as substrate for supporting, e.g., biomolecules.[7] Therefore, careful identification of these defects and measurement of their electronic effects so that a direct comparison with theory may become possible are motivations of this research.

In this paper, STM images of graphite samples are presented, in which the structures of two defects are determined, and their electronic effects are identified and measured. These results suggest that π states of graphite near the Fermi level have unexpectedly long intra- and interlayer correlation distances.

The STM used in this experiment is a modified "slip-stick" type of tip approach with a strong spring clamping of the tube-scanner unit. A detailed description of the STM design will be published elsewhere.[8] All STM images were taken in the constant current mode and in air ambient conditions. STM tips were mechanically formed from Pt90/Ir10 wires. Highly oriented pyrolitic graphite samples (Union Carbide, grade ZYH) were prepared by cleaving with an adhesive tape.

A hexagonal superlattice with periodicity 36 Å, superimposed on top of an atomic lattice of graphite (0001) plane with about 30° angle between their lattice vectors, was imaged on one of the samples. In particular, a "supervacancy" was found within the superlattice, as shown in Fig. 1(a). A dark valley with an area about 30 Å×30 Å is visible located at what was expected to be a bright peaking area for the superlattice. The image was taken with tunneling current set to 1 nA and bias voltage 125 mV, tip positive with respect to sample. The superlattice has a z corrugation about 0.6 Å with simultaneously obtained atomic corrugation about 0.35 Å [see cross-section plot Fig. 1(b)]. The z contrast between the dark valley and nearby superlattice peaks is ~1.5 Å. Interestingly, focusing inside the supervacancy, STM images [Fig. 1(c)] show an atomic point defect at the center of the dark valley. The atomic image of neighboring area shows a typical graphite (0001) surface undisturbed by the point defect, except a slight apparent outward (and upward) move for the direct neighboring atoms, which may be an electronic effect. Images of nearby regions show uniform superlattice, and no other defects were detected on the surface within a radius of at least 400 Å. These images strongly suggest that the observed point defect on the surface is responsible for the missing part of the superlattice, or the reduction of 1.5 Å in z height of an 30 Å×30 Å area.

The point defect shown in Fig. 1(c) appears as a missing lattice of ~1 Å hole depth. It is well known that holelike structures in a STM image can be caused by adsorbates that lower the density of states near the Fermi edge. One objection to such an explanation is that intentionally[9] or unintentionally[10] deposited foreign molecules have been found that did not cause any observable change of the underlying superlattices. (The origin of the superlattice will be discussed later.) That is also

0163-1829/94/50(3)/1839(5)/$06.00

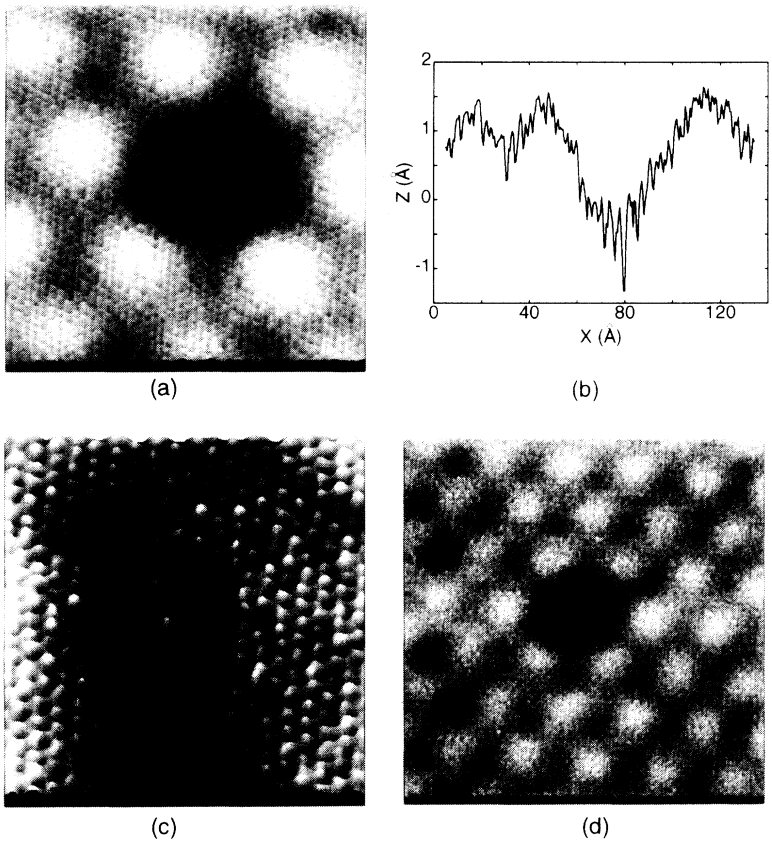

FIG. 1. (a) STM image showing a supervacancy in a superlattice of lattice spacing 36 Å on graphite (100 Å×100 Å, $V_{tip}=125$ mV, $I_t=1.0$ nA). Detailed structures in the dark region have some artifacts from smoothing, and should refer to (c). (b) A cross section of (a) from the lower-left corner to the upper-right corner. (c) An atomic vacancy at the center of the dark region of (a) (41 Å×41 Å, $\Delta Z=1.3$ Å, $V_{tip}=125$ mV, $I_t=1.0$ nA). (d) The same sample location as (a), after trapping an unknown molecule (206 Å×206 Å, $\Delta Z=1.0$ Å, $V_{tip}=200$ mV, $I_t=1.0$ nA).

confirmed on our sample by locating (after four days with STM sitting in the air) some molecules (contaminates) in a nearby superlattice region. Furthermore, after scanning an area containing both these molecules and the supervacancy in a fast scan mode, one of these molecules was trapped in the point defect while all the others disappeared from the scanned area. Figure 1(d) shows the same supervacancy as in Fig. 1(a), but with the trapped molecule which appears as an atomic protrusion. For images scanned with the same parameters, the size and depth of the supervacancy do not have any measurable change before and after the trapping of the molecule. The point defect in Fig. 1(c) acted as an atomic trap with the underlying supervacancy insensitive to its trapping-detrapping (protrusion-hole) status. These observations can hardly be reconciled with the explanation that the observed point defect is a result of adsorbates on a defect-free substrate. Besides adsorbates, point defects on graphite have never before been well characterized in an STM image. Point defects introduced by tip crashing, voltage pulse on bias[11] and ion bombardment[12] have shown damages on the nearby regions. However, the point defect of Fig. 1(c) is basically confined to one surface unit cell (one visible atomic position), which strongly suggests that the defect is an atomic vacancy (a missing atom).

Hexagonal superlattices on graphite have been reported by many groups.[9] The reported periodicity ranged from 17 to 440 Å, and they were usually terminated by sharp steps or twist boundaries. Kuwabara, Clarke, and Smith[13] suggested that the superlattice may be rotational Moiré patterns, where the topmost graphite (0001) sheet is rotated by a small angle with respect to the substrate. Therefore the superlattice periodicity D and the rotation angle θ are related as $D=d/[2\times\sin(\theta/2)]$, where $d=2.45$ Å is the atomic lattice spacing. This was recently confirmed by Xhie *et al.*,[9] and by Rong and Kuiper[14] through direct imaging of related atomic lattice vectors. Therefore, the superlattice shown in Fig. 1(a) is expected to have the same origin. By expanding the scan region, the area of Fig. 1(a) is found to be inside a ~1500-Å-wide strip [region C of Fig. 2(a)], which is terminated on both sides by sharp boundaries. The lower-right boundary is a two-step staircase with step sizes both about one atomic-layer height 3.5 Å. Images on the lowest region (A) show a typical graphite (0001) plane without superlattice. One atomic step up from region A, images on region B show the same superlattice as a continuation of region C except with much higher z corrugation [see solid line in Fig. 2(b)]. Since it has been established that the superlattice is a Moiré pattern due to a relative rotation between graphite planes, the continuation of the superlattice from region B to region C (with an attenuation) suggests that the rotation is between plane B and A rather than between plane B and C. The measurements of atomic lattice vectors of planes A, B, and C are also consistent with the suggestion. Therefore, images on region B can be called direct Moiré patterns [Fig. 3(a) is one of the examples] and images on region C can be called Moiré patterns covered by an overlayer. Near the upper-left corner of Fig. 2(a), the superlattice is terminated by a ~200-Å-wide band (region E) with a pair of beadlike chain edges

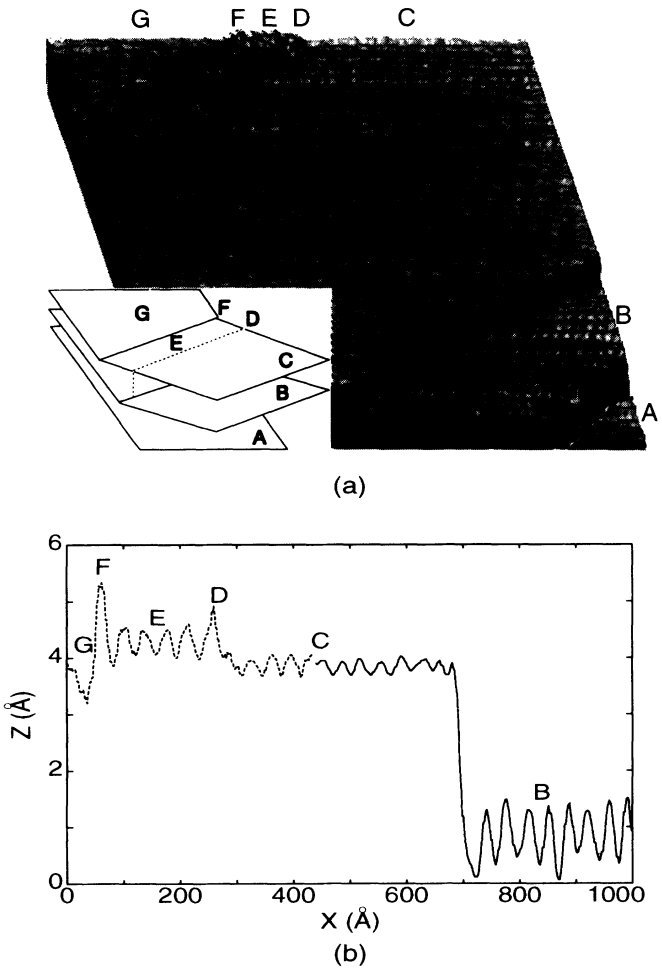

FIG. 2. (a) Large-scale STM image of the graphite sample (2030 Å×2030 Å, $V_{tip}=125$ mV, $I_t=1.0$ nA). Images in Fig. 1 were obtained from region *C*. The inset is a schematic model for the sample. (b) STM scan lines crossing regions *B* and *C* (solid line, $V_{tip}=20$ mV, $I_t=0.8$ nA), and the band near the upper-left corner of (a) (dashed line, $V_{tip}=180$ mV, $I_t=0.9$ nA).

(chain *D* and chain *F*, respectively). The two chains which extend several thousand angstroms, though relatively parallel, have no correlation in shape, and this excludes the multiple tip as an origin. The dashed line in Fig. 2(b) shows a cross section of the band. Inside the band (region *E*) the superlattice regains its high *z* corrugation to an amplitude roughly equal to those on region *B*. The left *F* chain is much higher than the right *D* chain. Atomic resolved images of chain *D* show an underlying graphite atomic lattice continuously across chain *D* without observable distortion. However, along chain *F*, STM images become very noisy and atomic resolution was not obtained, similar to those twist boundary terminations of Moiré patterns reported previously.[9,14] At the upper-left corner of Fig. 2(a), STM images show a normal graphite region (*G*).

Based on the above analysis, a three-layer model can be used to describe the sample system, a schematic drawing of which is shown as the inset of Fig. 2(a). Part of the top two graphite sheets (*B* and *C*) are rotated together by an angle $\theta=3.9°$ (calculated from the formula that relates angle to Moiré pattern periodicity) with respect to the underlying substrate (*A*). The rotated patch of plane *C* is terminated by a twist boundary at line *F*. The rotated patch of plane *B* is terminated by another twist boundary at line *D*. Therefore, images on region *E* show a direct Moiré pattern due to the relative rotation between the rotated part of plane *C* and the unrotated part of plane *B*. Chain *D* is the image of a twist boundary on the subsurface layer (*B*).

On a different graphite sample, we found another direct Moiré pattern, with a periodicity 66 Å [Fig. 3(b)]. The image shows bright peaks in a centered-hexagonal lattice, each surrounded by a hexagonal ring of six grayish valleys. This geometry can be visualized by overlaying two identical hexagonal patterns on transparencies and rotating one with respect to the other. The rotation creates three kinds of high-symmetry areas with local stacking orders *AAB*, *BAB*, and *CAB*, respectively. In a two-layer approximation, area *AAB* is surrounded by six equivalent *BAB* or *CAB* areas. Recent band-structure calculations[15] show that the density of states (DOS) at the Fermi level of simple hexagonal *AAA*-stacked graphite (0.0085 states/eV) is about three times higher than that of rhombohedral *CAB*-stacked (0.0021 states/eV) or normal hexagonal *AB*-stacked graphite (0.0033 states/eV). This is in agreement with the high peaking of area *AAB* (2.6 Å). Also, according to *ab initio* calculations, hypothetical graphite with *AA* stacking has virtually the same interlayer spacing as *AB*- and *CAB*-stacked graphite.[16] Therefore, the Moiré pattern is mainly an electronic

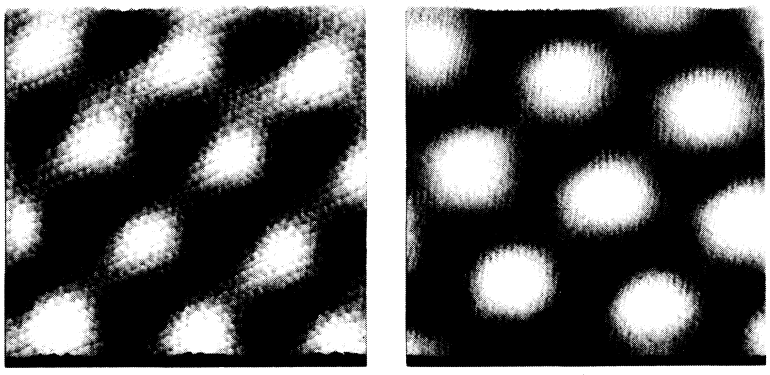

FIG. 3. STM images (a) on region *B* of Fig. 2(a) (100 Å×100 Å, $\Delta Z=1.7$ Å, $V_{tip}=15$ mV, $I_t=0.8$ nA), and (b) on a different graphite sample with a superlattice spacing 66 Å (202 Å×202 Å, $\Delta Z=2.3$ Å, $V_{tip}=72$ mV, $I_t=5.6$ nA).

effect rather than a real physical buckling, and detailed arguments were given previously.[14]

Concluding from the above analysis, the observed superlattices are rotational Moiré patterns, and their z contrasts are modulations on surface DOS from subsurface layers. In particular, in the image of Fig. 1(a), the modulation is from the third surface layer. The strength of this interlayer electronic coupling can be measured. Z corrugations of direct Moiré pattern are four times larger than simultaneously obtained atomic corrugations [Fig. 3(a) and Fig. 3(b)]. The attenuation of the Moiré pattern by an overlayer ($\mathcal{A} \equiv$ the ratio between corrugations of direct Moiré pattern and Moiré pattern covered by an overlayer) can be measured from the solid line ($\mathcal{A} \cong 2.6$, $V_{\text{tip}} = 20$ mV, $I_t = 0.8$ nA) and the dashed line ($\mathcal{A} \cong 2.3$, $V_{\text{tip}} = 180$ mV, $I_t = 0.9$ nA) in Fig. 2(b). It can also be obtained by a comparison between Fig. 3(a) and an image on region C ($\mathcal{A} \cong 2.6$, $V_{\text{tip}} = 15$ mV, $I_t = 0.8$ nA). The attenuation for the beadlike chain is about 1.6, measured from the dashed line of Fig. 2(b). (This is an underestimation due to the instrumental smoothing.) Considering the weak interlayer coupling of graphite, these attenuation factors are surprisingly low. An attenuation factor of 5 on Moiré pattern by two graphite overlayers was previously reported.[10] These possible low attenuation values suggest that Moiré pattern can propagate along the c axis through a few layers, especially for the beadlike string where huge amplitude is observed. These beadlike strings may be one of the sources for creating mysterious "DNA"-like images on graphite surface.[7] The effectiveness of screening by a single graphite layer, a common assumption for modeling graphite intercalation compounds, may need a rejustification.

The z corrugation of a direct Moiré pattern is voltage dependent, which increases when bias voltage is decreased, which was also found on the sample of Fig. 3(b).[14] The voltage dependence is stronger with the tip biased positively. However, the voltage dependence for the Moiré pattern covered by an overlayer is rather weak, which makes the attenuation voltage dependent. As the z corrugation at the atomic scale on graphite is tip dependent one might expect that the superstructure would be also. Under the single-tip assumption, the z corrugation of superlattice is virtually independent of tip material due to its large lattice vector.[17] However, interesting tip dependences of the z corrugation as well as the Moiré pattern shape were found when a multiple tip was identified. The multiple tip effect on superlattice is very similar to those on atomic scale images of graphite reported by Mizes, Park, and Harrison.[18]

The two Moiré patterns of Fig. 3(a) and Fig. 3(b) have very different shapes. Figure 3(a) shows a triangular pattern between three different regions with different brightness and is a typical image for those Moiré patterns with periodicity below 44 Å.[9,10] The Moiré pattern imaged on region B does not change shape with bias voltages (10 mV to 1 V) or bias polarities. Figure 3(b) shows a six-valley structure which surrounds every brightest peak and is a typical image for those Moiré patterns with periodicity above 66 Å.[13,14] In analyzing Fig. 3(b), we have treated the three high-symmetry areas as unrelated crystals with respective stacking sequences, and that matches well with available band-structure calculations.[14] However, the difference between Fig. 3(a) and Fig. 3(b) suggests that an intralayer correlation becomes important when the size of the Moiré pattern is reduced.

The above horizontally extended electronic influence can also be used to explain Fig. 1(a): the suppression of a Moiré pattern peaking area of 30 Å×30 Å by an atomic vacancy. It is very unlikely that a single atomic vacancy can cause such an 1.5-Å change in real z height on an atomic plane. Isolated adsorbed molecules are often found on graphite to be accompanied by $(\sqrt{3}\times\sqrt{3})R30°$ superlattices, which extends typically few tens of Å. Mizes and Foster[19] suggested that it is an oscillation caused by the scattering of the charge-density wave on a localized perturbation. Different from physi- or chemisorption, atomic vacancies on (0001) surface create extra dangling bonds, which may change the electronic structure of the surrounding area. More probably, the termination of these dangling bonds opened up a gap at the Fermi level for the half-filled π band, since that is likely to be stabilizing.[5] I suggest that the supervacancy indicates a lowering of DOS near the Fermi level caused by the atomic vacancy, an opposite effect to the AA stacking of the underlying layers, and the 30 Å×30 Å area is related to the intralayer correlation length of the π electron system. A thorough understanding requires further experimental and theoretical work.

In summary, electronic effects of two well-defined defects on a graphite sample were simultaneously imaged by STM. An atomic vacancy on the topmost (0001) plane caused a lowering of surface DOS in a 30 Å×30 Å area. It completely suppressed an expected higher DOS in the area due to the underlying AA stacking caused by a plane rotation with respect to the third surface layer. The rotational Moiré pattern has an attenuation factor ~ 2.6 per monolayer. These measurements may provide justification for modeling graphite related materials.

This work was supported by the Air Force Office of Scientific Research, AFOSR Grant No. F49620-92-J-0358.

[1] R. C. Tatar and S. Rabii, Phys. Rev. B **25**, 4126 (1982).
[2] J. Tersoff, Phys. Rev. Lett. **57**, 440 (1986).
[3] D. Tománek *et al.*, Phys. Rev. B **35**, 7790 (1987).
[4] J. Tersoff and D. R. Hamann, Phys. Rev. B **31**, 805 (1985); Phys. Rev. Lett. **50**, 1998 (1983).
[5] J. Robertson, Adv. Phys. **35**, 317 (1986).
[6] M. S. Dresselhaus and D. Dresselhaus, Adv. Phys. **30**, 139 (1981).
[7] C. R. Clemmer and T.P. Beebe, Science **251**, 640 (1991).
[8] Z. Y. Rong and L. Rokhinson, Phys. Rev. B **49**, 7749 (1994).

[9]See J. Xhie, K. Sattler, M. Ge, and N. Venkateswaran, Phys. Rev. B **47**, 15 835 (1993), and references therein.
[10]C.-Y. Liu, H. Chang, and A. J. Bard, Langmuir **7**, 1138 (1991).
[11]Phys. Today **41** (5), 129 (1988).
[12]G. M. Shedd and P. E. Russell, J. Vac. Sci. Technol. A **9**, 1261 (1991).
[13]M. Kuwabara, D. R. Clarke, and D. A. Smith, Appl. Phys. Lett. **56**, 2396 (1990).
[14]Z. Y. Rong and P. Kuiper, Phys. Rev. B **48**, 17 427 (1993).
[15]J.-C. Charlier, J.-P. Michenaud, and Ph. Lambin, Phys. Rev. B **46**, 4540 (1992).
[16]J.-C. Charlier, J.-P. Michenaud, and X. Gonze, Phys. Rev. B **46**, 4531 (1992).
[17]J. Tersoff, Phys. Rev. B **41**, 1235 (1990); J. Tersoff and N. D. Lang, Phys. Rev. Lett. **65**, 1132 (1990).
[18]H. A. Mizes, Sang-il Park, and W. A. Harrison, Phys. Rev. B **36**, 4491 (1987).
[19]H. A. Mizes and J. S. Foster, Science **244**, 559 (1989).

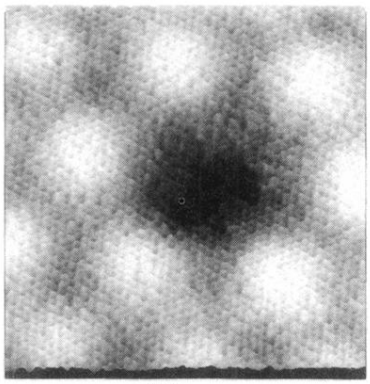

(a)

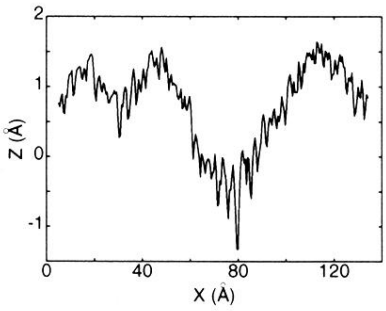

(b)

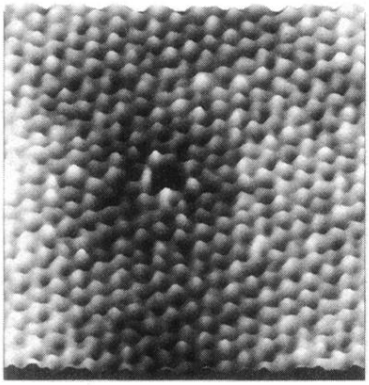

(c)

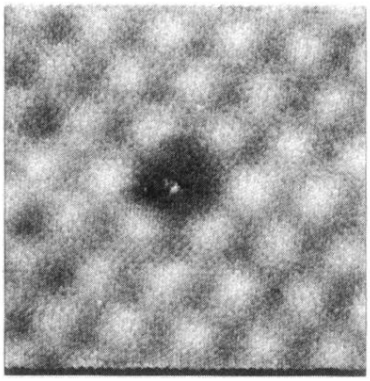

(d)

FIG. 1. (a) STM image showing a supervacancy in a superlattice of lattice spacing 36 Å on graphite (100 Å×100 Å, $V_{tip}=125$ mV, $I_t=1.0$ nA). Detailed structures in the dark region have some artifacts from smoothing, and should refer to (c). (b) A cross section of (a) from the lower-left corner to the upper-right corner. (c) An atomic vacancy at the center of the dark region of (a) (41 Å×41 Å, $\Delta Z=1.3$ Å, $V_{tip}=125$ mV, $I_t=1.0$ nA). (d) The same sample location as (a), after trapping an unknown molecule (206 Å×206 Å, $\Delta Z=1.0$ Å, $V_{tip}=200$ mV, $I_t=1.0$ nA).

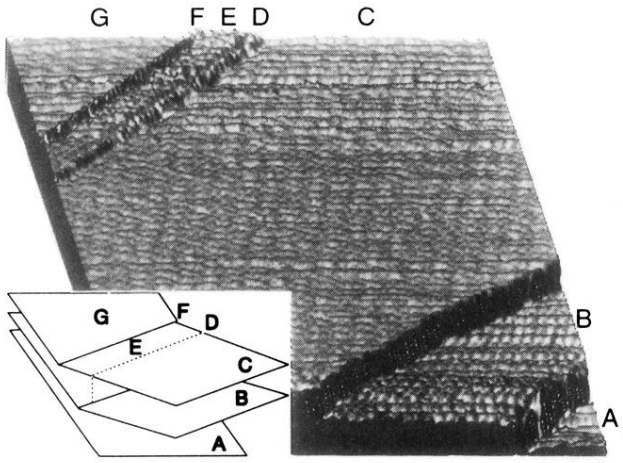

(a)

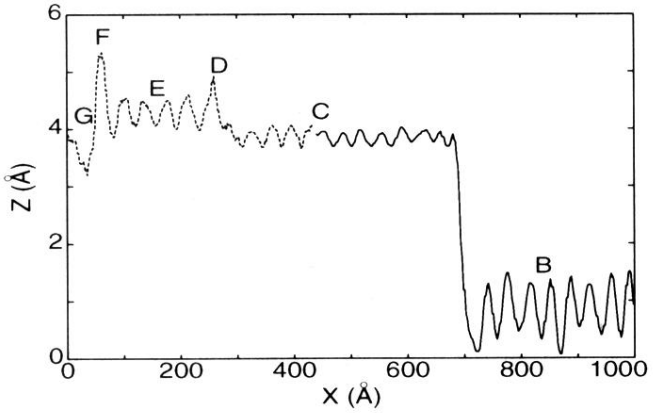

(b)

FIG. 2. (a) Large-scale STM image of the graphite sample (2030 Å×2030 Å, $V_{tip}=125$ mV, $I_t=1.0$ nA). Images in Fig. 1 were obtained from region *C*. The inset is a schematic model for the sample. (b) STM scan lines crossing regions *B* and *C* (solid line, $V_{tip}=20$ mV, $I_t=0.8$ nA), and the band near the upper-left corner of (a) (dashed line, $V_{tip}=180$ mV, $I_t=0.9$ nA).

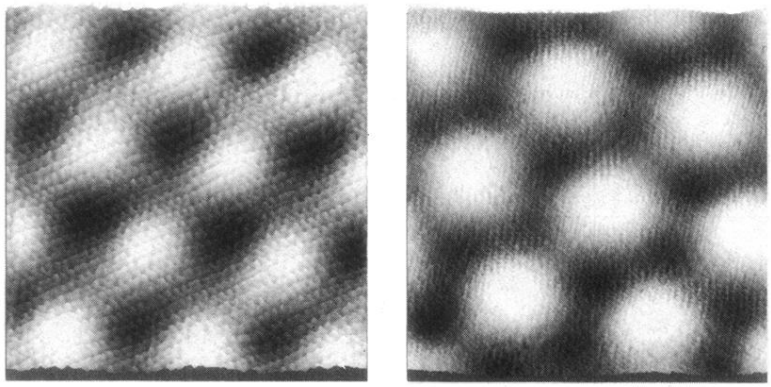

(a) (b)

FIG. 3. STM images (a) on region B of Fig. 2(a) (100 Å × 100 Å, $\Delta Z = 1.7$ Å, $V_{\text{tip}} = 15$ mV, $I_t = 0.8$ nA), and (b) on a different graphite sample with a superlattice spacing 66 Å (202 Å × 202 Å, $\Delta Z = 2.3$ Å, $V_{\text{tip}} = 72$ mV, $I_t = 5.6$ nA).